

Sec. III, the procedure is five or six times faster than standard (noniterative) methods now in use to solve the same equations.¹⁷ If the S matrix is desired as a function of energy, the Fredholm method is even more advantageous. Most of the time in the calculations reported here is spent in computation of the matrix elements; since a large proportion of these matrix elements do not need to be recalculated as the scattering energy is varied, the method becomes relatively more efficient for each succeeding energy. Thus, in

the case that scattering information is desired over a range of energies—for example, near a resonance or threshold—it seems safe to say that the method is at least an order of magnitude faster than other methods presently in use.

ACKNOWLEDGMENT

The author is grateful to Attila Szabo for numerous discussions concerning the Fredholm method, and for carrying out the optical-potential calculation presented in Sec. IV.

¹K. J. LeCouteur, Proc. Roy. Soc. (London) A256, 115 (1960).

²R. G. Newton, J. Math. Phys. 2, 188 (1961).

³R. Blankenbecler, in *Strong Interactions and High Energy Physics*, edited by R. G. Moorehouse (Oliver and Boyd, Edinburgh, 1964); R. Sugar and R. Blankenbecler, Phys. Rev. 136, B472 (1965).

⁴R. G. Newton, J. Math. Phys. 8, 2347 (1967).

⁵W. P. Reinhardt and A. Szabo, Phys. Rev. A 1, 1162 (1970). This paper will be referred to in the text as I. I contains a brief review of previous applications of the Fredholm method to one-channel problems.

⁶See, for example, N. F. Mott and H. S. W. Massey, *The Theory of Atomic Collisions*, 3rd ed. (Oxford U. P., London, 1965), p. 388. What we call the R matrix is often called the K matrix: See, for example, R. G. Newton, *Scattering Theory of Waves and Particles* (McGraw-Hill, New York, 1966), p. 190.

⁷M. Baker, Ann. Phys. (N. Y.) 4, 27 (1958). Note that in I the exponents $(2l+1)$ were inadvertently omitted from the partial-wave expansion of the full determinant.

⁸We are following the notation of Newton, Refs. 2 and 4.

⁹In order to simplify the notation we have assumed that (a) all the η channels are open, (b) in each channel the integration over momenta is approximated by an n -point numerical quadrature, and (c) the dimension of our determinant is thus $N+n\eta$ when $N=n\eta$. These conventions are

adopted purely for notational simplification—in an actual calculation all can be violated.

¹⁰J. H. Wilkinson, *The Algebraic Eigenvalue Problem* (Clarendon, Oxford, 1965), Chap. 4.

¹¹That is, after a symmetric matrix has been partially triangularized, the remaining portion is still symmetric.

¹²This is made clear by the realization that application of the substitution rules to $\det(1-iR)$ yields the same S -matrix elements as would be obtained by directly inverting $(1-iR)$ and constructing S as $(1+iR)(1-iR)^{-1}$, the only ambiguity being in the signs of off-diagonal S -matrix elements. This result gives an interesting insight into the actual mechanism of operation of the substitution rules, which otherwise seem slightly mysterious.

¹³P. G. Burke and K. Smith, Rev. Mod. Phys. 34, 458 (1962); see also S. Geltman, *Topics in Atomic Collision Theory* (Academic, New York, 1969), Sec. 16, for a straightforward development of these potentials.

¹⁴See Ref. 10. The partial pivoting is, of course, restricted to the first N rows of the determinant.

¹⁵H. Feshbach, Ann. Phys. (N. Y.) 5, 357 (1958); 19, 287 (1962); L. Fonda and R. G. Newton, *ibid.* 10, 490 (1960).

¹⁶R. J. Huck, Proc. Phys. Soc. (London) A70, 369 (1957).

¹⁷S. Geltman (private communication).

Excitation of the $(2p^2)^3P$ State of Helium near Threshold*

P. D. Burrow

Mason Laboratory, Yale University, New Haven, Connecticut 06520

(Received 29 June 1970)

The trapped-electron method is applied to the excitation by electron impact of the $(2p^2)^3P$ state, the lowest doubly excited state of helium which is stable against auto-ionization. The energy of this state, 59.64 ± 0.08 eV, is in good agreement with theory. An estimate of the slope of the total cross section for excitation of the $(2p^2)^3P$ state at threshold gives a value of 4×10^{-20} cm²/eV.

INTRODUCTION

Certain of the doubly excited states of helium have properties which make their observation difficult.

These states, such as the $(2p^2)^3P$, $(2p3p)^1P$, and 3P states, possess even parity but odd orbital angular momentum. They cannot be detected by a photo-absorption technique such as that used by Madden

and Codling¹ because optical transitions from the ground state are forbidden. Auto-ionization of these doubly excited states, resulting in a positive ion and a free electron, is also forbidden. The selection rules for auto-ionization require both the parity and the orbital angular momentum, in the LS coupling scheme, to remain unchanged. Because the helium ion is in the 2S state, the ejected electron must possess even parity but odd angular momentum, and these conflicting requirements forbid the auto-ionization transition. The states listed above, therefore, cannot be observed by energy analysis of the ejected electron as used by Rudd.²

Becker and Dahler³ have calculated the angular distribution of the scattered electrons resulting from excitation by electron impact of the doubly excited non-auto-ionizing states. They found that the outgoing electron emerges preferentially at right angles to the incoming beam and that there is no scattering in the forward direction. This property of the "parity-unfavored" transitions has been discussed in more general terms by Fano.⁴ Since previous studies of the excitation of doubly excited states by electron impact have been done by observation of scattering in the forward direction, states having even parity and odd angular momentum could not be observed.⁵

In the present experiment the trapped-electron method⁶ is used to study the excitation of the lowest non-auto-ionizing doubly excited state in helium, the $(2p^2)^3P$ state, near its threshold.

APPARATUS

The trapped-electron method provides a sensitive technique for the complete collection of slow electrons resulting from inelastic collisions. The collection mechanism is independent of the scattering angle, and thus the current of trapped electrons is proportional to the total inelastic cross section. Because of the high collection efficiency of the trapped-electron method, it is suitable for the study of excitation cross sections near their thresholds.

Figure 1 shows a schematic diagram of the tube and the variation of potential along the axis. An electron beam, collimated by a magnetic field of about 250 G, is accelerated into the collision chamber with voltage V_A . The collision chamber consists of two end plates and a grid formed by ten wires, 0.007-cm diam, strung longitudinally and spaced equally around a circle. A cylindrical outer collector, marked trapped-electron collector in Fig. 1, surrounds the collision chamber. By applying a positive voltage to this collector with respect to the collision chamber, an electrostatic well, having depth WV , can be produced along the axis of the tube.

An electron making an inelastic collision just

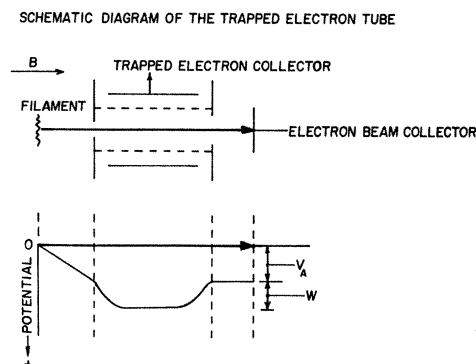


FIG. 1. Schematic diagram of the trapped-electron tube and the potential distribution along the axis of the tube. The accelerating voltage is given by V_A and the depth of the well by W .

above the threshold for an inelastic process loses most of its energy and is trapped in the well. It spirals back and forth following the magnetic field lines and eventually makes enough elastic collisions to diffuse across the magnetic field to the trapped-electron collector. At an energy W eV above the threshold of an inelastic process, the electrons have enough energy remaining to escape through the potential barrier at the end of the collision chamber, and the trapped-electron current vanishes. Therefore, as a function of accelerating voltage, the trapped-electron current is zero below an inelastic threshold and then grows to a peak which is proportional to the magnitude of the cross section at an energy W eV above the threshold.

The well depth is determined by applying a negative voltage to the trapped-electron collector relative to the collision chamber, thus creating a potential barrier in the path of the electron beam. By measuring the shift in the electron beam retarding curve for different values of the applied voltage, the size of the barrier is determined. This is the well depth with reversed polarity.

The tube is constructed of Advance metal and molybdenum grid wires. All metal parts are gold plated to avoid contact potential shifts. The electron gun consists of a thoria-coated iridium filament and three accelerating plates (not shown in Fig. 1). The retarding potential difference method⁷ is used to produce an electron beam with 0.1–0.2-eV width at half-maximum. The tube is mounted in a stainless-steel envelope, and externally mounted Helmholtz coils provide the collimating magnetic field. The tube and vacuum system are baked at 400°C and reach a background pressure of 1×10^{-9} Torr. Reagent-grade gases from high-pressure bottles supplied by the J. T. Baker Chemical Company are used. Continuous flow of the gas is maintained in order to minimize the buildup of impurity gases in the collision chamber. The pressure in

the collision chamber is typically 4×10^{-3} Torr.

In the present application, the electron impact energy is considerably above the first ionization potential of helium. The positive ions which are produced have thermal energies and cannot reach the trapped-electron collector which is typically biased several tenths of a volt positive with respect to the collision chamber. The ions, therefore, are collected at the end plates of the collision chamber or leave through the entrance and exit holes. The positive space charge produced by the ions appears to have little effect on the well depth in the collision chamber. This point was checked by observing excitation to the singly excited states of helium with and without an argon ion background.

Operation above the first ionization potential produces a large background current of slow electrons due to direct ionization. In helium this current is approximately constant in the range of impact energies studied here and is largely suppressed.

The trapped-electron current is measured with a vibrating-reed electrometer. The output of the electrometer is stored and averaged in a multi-channel analyzer.

RESULTS

Figure 2 shows the trapped-electron current in helium as a function of electron impact energy in the region near 60 eV. The well depth is 0.11 V. Peaks due to the excitation of the four lowest doubly excited states are shown. These are superposed on the background current of slow electrons resulting from direct ionization. Three of the four

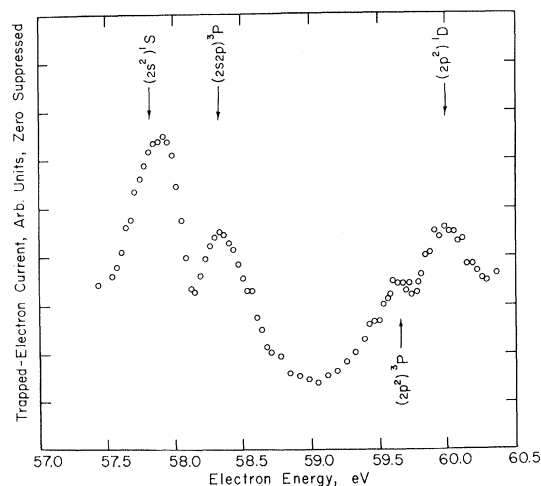


FIG. 2. The trapped-electron current in helium as a function of electron impact energy near 60 eV. The well depth is 0.11 V. The background current of slow electrons resulting from direct ionization is suppressed. Calibration of the energy scale is discussed in the text. In this figure, the energy scale is shifted so that the threshold for excitation of the $(2s2p)^3P$ state appears at the maximum of the corresponding peak in the trapped-electron current.

peaks in Fig. 2 correspond to the three lowest doubly excited states which are unstable with respect to auto-ionization. In order of increasing energy, these are the $(2s^2)^1S$, $(2s2p)^3P$, and the $(2p^2)^1D$ states. They have been previously studied by energy-loss measurements of forward-scattered electrons⁵ and by positive ion^{2,8} and electron⁹ impact followed by analysis of the ejected electron, and their energies are well known. All three states are optically forbidden from the ground state.

The second-lowest doubly excited state, designated $(2s2p)^3P$, is used for calibration of the energy scale. Rudd² has calibrated this state, within ± 0.05 eV, against one of the optically allowed doubly excited states measured with great accuracy by Madden and Codling.¹ Rudd's value for the energy of the $(2s2p)^3P$ state is also in good agreement with the theoretical value calculated by Burke.¹⁰ Because of the short lifetime of an auto-ionizing state, its energy measured experimentally may be uncertain within an amount roughly equal to the spread in energy introduced by the decay process. In general, the lifetimes of the states in helium correspond to widths in energy which are considerably smaller than the half-width of the electron-beam energy distribution. The error in the measured energy due to the lifetime is usually negligible. A notable exception is the lowest doubly excited $(2s^2)^1S$ state, which has a calculated width of 0.124 eV.¹⁰ The increased width broadens the energy range over which slow electrons are produced near threshold. In data taken with higher-energy resolution,¹¹ the peak in the trapped-electron current due to excitation of the $(2s^2)^1S$ state exhibits a width at half-maximum which is increased by 0.08 eV over that for excitation to the $(2s2p)^3P$ state. The latter state has a calculated width¹⁰ of only 0.009 eV and is better suited for energy calibration.

For convenience of display, the energy scale in Fig. 2 is positioned so that the threshold for excitation of the $(2s2p)^3P$ appears at the maximum of the corresponding peak in the trapped-electron current. The actual threshold lies to the left of the maximum by an amount approximately equal to the well depth.¹² Because the energies of the other states are measured relative to that of the $(2s2p)^3P$ state, it is more accurate to refer to the positions of the maxima. Using this calibration procedure, the arrows at the top of Fig. 2 indicate the positions of the other auto-ionizing states as given by Rudd.^{2,8}

The small peak at 59.64 ± 0.08 eV is attributed to the $(2p^2)^3P$ state, the lowest of the doubly excited non-auto-ionizing states. Wu¹³ has given a strong argument that dipole radiation from this state to the $(1s2p)^3P$ state could account for the vacuum ultraviolet line at 320.392 \AA observed by Compton and Boyce¹⁴ and by Kruger.¹⁵ The sum of

TABLE I. Energies of the four lowest doubly excited states of helium, energy in eV.

Doubly excited state	Rudd ^a	Oda, Nishimura, and Tahira ^b	Present work	Burke ^c	Spectroscopic ^d	Holøien ^e	Drake and Dalgarno ^f
$(2s^2)^1S$	57.82	57.9	57.89	57.84			
$(2s2p)^3P$	58.34	58.3	58.34 ^g	58.32			
$(2p^2)^3P$			59.64		59.659	59.682	59.671
$(2p^2)^1D$	60.0 ^h	59.9	59.95	59.91			

^aReference 2.^bReference 9.^cReference 10.^dReference 16.^eReference 17.^fReference 18.^gRudd's value for the energy of the $(2s2p)^3P$ state is used for calibration of the energy scale.^hReference 8.

the energies of the $(1s2p)^3P$ and the 320.392-Å emission line yield an energy of 59.659 eV for the $(2p^2)^3P$ state.¹⁶ This value is in very good agreement with the energy measured here, namely, 59.64 eV. Theoretical values for the energy of the $(2p^2)^3P$ state fall well within the range of error of the present experiment. Calculations of Holøien¹⁷ and Drake and Dalgarno¹⁸ yield energies of 59.682 and 59.671 eV, respectively.

A summary of the measured and calculated energies of the four lowest doubly excited states of helium is given in Table I. The experimental error in the present data is ± 0.08 eV.

An estimate of the cross section for the excitation of the $(2p^2)^3P$ state at 0.11 eV above its threshold may be made from the trapped-electron data. The height of the corresponding peak in the trapped-electron current, measured above the continuum background, is proportional to the desired cross section. An absolute value is obtained by calibrating this peak height against that for excitation to the $(1s2s)^3S$ metastable level in helium measured under the same experimental conditions. The cross section near threshold for this latter state is known from several measurements.¹⁹ The calibration procedure yields a total cross section of 4.4×10^{-21} cm² for excitation of the $(2p^2)^3P$ state at 0.11 eV above threshold. Assuming a linear dependence on energy, the cross section possesses a slope of 4×10^{-20} cm²/eV at threshold. Because the peak for the $(2p^2)^3P$ state is not well resolved from that for the next higher state, the cross section is reliable only within a factor of 2.

Becker and Dahler³ have calculated the cross section for excitation of the $(2p^2)^3P$ state by several methods. The most reliable of these is expected to be the two-state strong-coupling approximation. The calculation is most appropriate for the determination of the maximum value of the cross section and its general dependence on energy rather than the threshold behavior. Nevertheless, it provides an estimate of the cross section to be expected on theoretical grounds. Their calculation gives a

slope at threshold of 5.6×10^{-21} cm²/eV. The experimental value measured here is larger by a factor of about 7. This discrepancy does not appear excessive considering the experimental error and the difficulty of calculating cross sections close to their thresholds.

Becker and Dahler also calculated cross sections for excitation to several non-auto-ionizing states lying at higher energies. All of these cross sections were smaller than that of the $(2p^2)^3P$ state by several orders of magnitude. No attempt was made to observe these higher states experimentally.

Experimental cross sections for the three remaining states shown in Fig. 2 are not obtainable from the present trapped-electron data. Because these states are unstable with respect to auto-ionization, they perturb the background continuum of states in their vicinity, and the number of slow electrons produced in direct ionization is changed. The magnitudes of the peaks in the trapped-electron current, therefore, are not easily interpreted. The characteristics of the line profiles of the auto-ionizing states have been discussed by Fano²⁰ and Fano and Cooper.²¹ In general, a line may have a portion rising above the continuum background and a portion dipping down into the continuum. For auto-ionizing states having widths narrower than the electron-beam energy distribution, the trapped-electron current arises from excitation of an average over the line profile. Profiles which have equal parts above and below the continuum background may appear only weakly, if at all, in the trapped-electron current. In a similar way, profiles consisting predominantly of a dip into the background may result in a dip in the trapped-electron current rather than a peak. The profiles of the optically forbidden levels discussed here were previously observed⁵ in electron scattering experiments, in which these states appeared in the energy-loss spectrum predominantly as peaks above the continuum when averaged over a beam half-width of 0.1 eV. This line shape is consistent with the peaks observed in the present experiment.

ACKNOWLEDGMENT

The author is indebted to G. J. Schulz, who col-

laborated on an earlier part of this work, for many useful discussions.

*Work supported by the National Science Foundation.

- ¹R. P. Madden and K. Codling, *Astrophys. J.* **141**, 364 (1965).
²M. E. Rudd, *Phys. Rev. Letters* **13**, 503 (1964); **15**, 580 (1965).
³P. M. Becker and J. J. Dahler, *Phys. Rev.* **136**, A73 (1964).
⁴U. Fano, *Phys. Rev.* **135**, B863 (1964).
⁵J. A. Simpson, S. R. Mielczarek, and J. Cooper, *J. Opt. Soc. Am.* **54**, 269 (1964); J. A. Simpson, G. E. Chamberlain, and S. R. Mielczarek, *Phys. Rev.* **139**, A1039 (1965).
⁶G. J. Schulz, *Phys. Rev.* **112**, 150 (1958); **116**, 1141 (1959).
⁷R. E. Fox, W. M. Hickam, D. J. Grove, and T. Kjeldaa, *Rev. Sci. Instr.* **26**, 1101 (1955).
⁸M. E. Rudd and D. V. Lang, in *Proceedings of the Fourth International Conference on the Physics of Electronic and Atomic Collisions* (Science Bookcrafter, Hastings-on-Hudson N. Y., 1965), p. 153.
⁹N. Oda, F. Nishimura, and S. Tahira, *Phys. Rev. Letters* **24**, 42 (1970).
¹⁰P. G. Burke, in *Advances in Atomic and Molecular Physics*, edited by D. R. Bates and I. Estermann (Aca-

demic, New York, 1968), Vol. 4, p. 209.

- ¹¹P. D. Burrow and G. J. Schulz, *Phys. Rev. Letters* **22**, 1271 (1969).
¹²The threshold lies to the left of the maximum in the trapped-electron current by an energy which depends on the magnitude of the well depth relative to the half-width of the electron-beam energy distribution.
¹³Ta-You Wu, *Phys. Rev.* **66**, 291 (1944).
¹⁴K. T. Compton and J. C. Boyce, *J. Franklin Inst.* **205**, 497 (1928).
¹⁵P. G. Kruger, *Phys. Rev.* **36**, 855 (1930).
¹⁶W. C. Martin, *J. Res. Natl. Bur. Std. (U.S.)* **A64**, 19 (1960).
¹⁷E. Holøien, *Phys. Norvegica* **1**, 53 (1961).
¹⁸G. W. F. Drake and A. Dalgarno, *Phys. Rev. A* **1**, 1325 (1970).
¹⁹G. J. Schulz and R. E. Fox, *Phys. Rev.* **106**, 1179 (1957); P. D. Burrow and G. J. Schulz, *ibid.* **187**, 97 (1969). A slope of $1.6 \times 10^{-17} \text{ cm}^2/\text{eV} \pm 30\%$ at threshold for excitation of the $(1s2s)^3S$ state is assumed for the calibration.
²⁰U. Fano, *Phys. Rev.* **124**, 1866 (1961).
²¹U. Fano and J. W. Cooper, *Phys. Rev.* **137**, A1364 (1965).

Vibrational Excitation in Electronically Excited Ions Produced by Charge Exchange

Michael J. Haugh* and Kyle D. Bayes

Department of Chemistry, University of California, Los Angeles, California 90024

(Received 16 March 1970)

The charge-exchange reactions between Ar^+ or Kr^+ and several molecules have been studied spectroscopically. Light emission is observed from the molecular ions, indicating near-resonant charge exchange. Measurements on mixtures of gases provide relative cross sections for the formation of electronically excited ions. The cross sections are largest for the smallest energy defect, in agreement with the theory of Rapp and Francis. The Franck-Condon principle is not a dominant factor in determining the populations of different vibrational levels of diatomic ions, but it may be important for triatomic ions.

INTRODUCTION

Charge exchange, the transfer of an electron from one atom or molecule to another, may result in an electronically excited product. If done in the gas phase at low pressure, the excited molecule will normally emit radiation before undergoing a collision. Spectroscopic analysis of that radiation can then provide direct information about the energy states of the products. This method has been used to investigate the electronic, vibrational, and rotational excitation of the newly formed ions.¹⁻⁸

When the charge transfer is resonant, for example, between H^+ and H, the cross section may

be quite large. As the relative velocity of the two particles increases, the cross section for charge exchange decreases. For nonresonant collisions, for example, between Ar^+ and Ne, the cross section for charge exchange is small at low velocities, but increases at higher velocities. At sufficiently high velocities, the cross sections are similar to those of resonant charge exchange.^{9,10} Most of the collisions in this work involve sufficiently high velocities so that near-resonant collisions are involved.

The velocity v at which the nonresonant collision attains a resonantlike cross section is given by the Massey adiabatic criterion¹¹